J Mater Sci: Mater Med (2010) 21:451–461
DOI 10.1007/s10856-009-3910-2

Influence of telopeptides, fibrils and crosslinking on physicochemical properties of Type I collagen films

Robin S. Walton · David D. Brand · Jan T. Czernuszka

Received: 22 July 2009 / Accepted: 8 October 2009 / Published online: 23 October 2009
© Springer Science+Business Media, LLC 2009

Abstract Type I collagen is widely used in various different forms for research and commercial applications. Different forms of collagen may be classified according to their source, extraction method, crosslinking and resultant ultrastructure. In this study, afibrillar and reconstituted fibrillar films, derived from acid soluble and pepsin digested Type I collagen, were analysed using Lateral Force Microscopy (LFM), Fourier Transform Infra-Red Spectroscopy (FTIR), Differential Scanning Calorimetry (DSC) and enzymatic stability assays to asses the influence of telopeptides, fibrils and crosslinking. LFM proved to be a useful technique to confirm an afibrillar/fibrillar ultrastructure and to elucidate fibril diameters. FTIR has proved insensitive to ultrastructural differences involving telopeptides and fibrils. DSC results showed a significant increase in T_d for crosslinked samples (+22–28°C), and demonstrated that the thermal behaviour of hydrated, afibrillar films is more akin to reconstituted fibrillar films than monomeric solutions. The enzymatic stability assay has provided new evidence to show that afibrillar films of Type I collagen can be significantly more resistant to collagenase (by up to 3.5 times), than reconstituted fibrillar films, as a direct consequence of the different spatial arrangement of collagen molecules. A novel mechanism for this phenomenon is proposed and discussed. Additionally, the presence of telopeptide regions in afibrillar tropocollagen samples has been shown to increase resistance to collagenase by greater than 3.5 times compared to counterpart afibrillar atelocollagen samples. One-factor ANOVA analysis, with Fisher's LSD post-hoc test, confirms these key findings to be of statistical significance ($P < 0.05$). The profound physicochemical effects of collagen ultrastructure demonstrated in this study reiterates the need for comprehensive materials disclosure and classification when using these biomaterials.

R. S. Walton (✉) · J. T. Czernuszka
Department of Materials, Oxford University, Oxford, UK
e-mail: robin.walton@materials.ox.ac.uk

D. D. Brand
Research Svc, VA Medical Center, Memphis, TN, USA

1 Introduction

Collagen is widely used in biomedical research as well as commercially in medical devices and cosmetic products [1–4]. One major biomedical use of collagen is in tissue engineering where porous, three-dimensional scaffold structures may be fabricated to provide a support structure for cells [5]. The most commonly utilized collagen, by far, is Type I, which may be extracted from animal sources (e.g. bovine [6], porcine [7] and equine [8]), from which the tissue may be of mature, immature or foetal origin. Collagen may also be extracted from human sources (cadavers/placenta/amnion [9]) or may be synthesized using recombinant genetic engineering techniques [10]. The collagen source, extraction method and post-processing used will result in collagenous material with a defined ultrastructure. The word ultrastructure used in this context refers to the presence or absence of telopeptides, the nature of fibrils (if present), and the type and extent of crosslinking. This study aims to investigate how ultrastructure influences the properties of collagen Type I films, using various physicochemical analytical techniques.

Currently, the vast majority of collagen Type I materials for research and commercial use are fabricated from animal tissue derivatives. Extraction from animal tissues often involves one of the following standard techniques: pepsin

digestion—to release soluble monomeric atelocollagen that is devoid of terminal telopeptides [11, 12], acid solubilization—to liberate monomeric tropocollagen with telopeptides intact [13, 14], or mucopolysaccharide and soluble protein cleansing of tissues rich in collagen Type I—to give insoluble, polymeric, naturally-crosslinked tropocollagen [15–17]. Monomeric tropocollagen, however, may only be liberated from immature or foetal tissues that have a minimal amount of inter-molecular crosslinking, much of which includes the telopeptide domain [18, 19]. It should be noted that in reality, a fully monomeric solution is almost impossible to be achieved—despite advancements in protein purification, there will almost certainly be a small contingent of dimeric, trimeric and polymeric triple-helix associations. However, for the purpose of this study, such near-monomeric solutions shall be referred to as "monomeric".

Post-extraction, monomeric collagens may be re-polymerized in vitro when subjected to physiological conditions through entropy-driven self-assembly (known as *fibrillogenesis*) [20]. This polymerization process results in reconstituted fibrils, stabilized by hydrogen bonds, that exhibit the characteristic 67 nm banding pattern of native collagen in tissues [21]. However, in the case of atelocollagen, proteolytic removal of telopeptides has been shown to drastically alter the in vitro self-assembly process [22, 23]. This results in raised nucleation energy, and a lengthened lag phase, to form fibrils with a less perfect packing order [23–25]. A recent study by Zeugolis et al. notes that "There is limited literature available on the factors which control the biophysical characteristics of reconstituted collagen fibers *prior* to fiber formation" [26]. This highlights the need for physicochemical data from Type I collagens with different ultrastructures, both pre and post fibril formation.

In commercial usage, atelocollagen is preferred due to the associated cross-species antigenicity of the p-determinant located in the telopeptides of animal-derived collagen [27]. The atelocollagen is often used in monomeric form in cosmetic make-up products, and in polymeric form for cell scaffolds/hemostats. Tissue augmentation procedures, for example, use an atelocollagen suspension stored at 4°C in physiologic saline so that any dispersed fibrils remain fluid and small. This enables the suspension to be directly injected into the augmentation site, upon which human body temperature drives the fibrillogenesis process [28]. Recently, however, because of the reported poor quality fibrils [23–25], and non-native structure of atelocollagen, there is increasing interest in the academic world in the properties of tropocollagens.

Further processing of collagen often involves a crosslinking step to increase mechanical strength and resistance to enzymatic degradation [29]; this is a crucial consideration when designing a collagen-based implant for tissue engineering. There are various methods available to crosslink collagen. These methods may be summarized as chemical, physical or biological; some of which, however, have been shown to have negative aspects to the treatment [30–36]. These side effects could have a negative influence on attachment, migration and proliferation of cells on collagenous biomaterials. Consequently, treatment with 1-ethyl-3-(3-dimethylaminopropyl)-carbodiimide/*N*-hydroxysuccinimide (EDC/NHS) has become a favourable method for collagen crosslinking as it has been shown to have good biocompatibility, increase the mechanical strength and increase the resistance of collagen to enzymatic degradation [37, 38].

To quantify the influence ultrastructure has on the properties of Type I collagen, suitable analytical and characterisation methods must be implemented. Atomic Force Microscopy (AFM) can be used to gather visual evidence of afibrillar/fibrillar ultrastructures and to determine fibril diameters, which has been shown to correlate with resistance to mechanical deformation at low strain rates [39]. Fourier Transform Infra-Red Spectroscopy (FTIR) is a useful method to monitor changes in secondary structure of a protein; in particular, changes in the amide A (3,400–3,450 cm^{-1}), amide I (1,636–1,661 cm^{-1}), amide II (1,549–1,558 cm^{-1}) and amide III (1,200–1,300 cm^{-1}) regions. Studies have shown that there may be changes in these regions when moving from a monomeric to a fibrillar ultrastructure [40–43], with crosslinking [44] and where denaturation occurs [32, 45]. Differential Scanning Calorimetry (DSC) is often used in collagen research to infer the level of crosslinking within a given sample through elucidation of its denaturation temperature (T_d) [46–48]. A higher denaturation temperature often infers a higher level of crosslinking which is expected to show a greater resistance to enzymatic degradation [37]. A standard laboratory test to determine enzymatic stability is the use of bacterial collagenase from *Clostridium histolyticum*. This matrix metallo-protease Type I (MMP1) enzyme is capable of cleaving more than 100 sites on each collagen α-chain [34]. However, studies show that this type of enzyme locally unwinds the triple helix of collagen first, then preferentially cleaves all the α-chains in a single scission at the Gly^{775}-Ile^{776} of α1 and Gly^{775}-Leu^{776} of α2 [49–51]. Understanding the mechanism of degradation is of great importance in the design of collagen biomedical devices where a predictable rate of degradation in vivo is desirable [52]. It should be noted though, that the specificity of mammalian collagenase is more limited than that of bacterial collagenase [53]. However, a good empirical correlation between the extent of in vitro degradation by bacterial collagenase, and in vivo degradation by mammalian collagenase, has previously been shown [54].

The principal goal of this study was to evaluate the differences between the properties of Type I acid solubilized tropocollagen and pepsin digested atelocollagen in the form of afibrillar and reconstituted fibrillar films, with and without EDC/NHS crosslinking. The rationale being to correlate any observed differences in properties to ultrastructural differences involving telopeptides, fibrils and crosslinking.

2 Materials and methods

2.1 Collagen sample preparation

Acid-soluble Type I tropocollagen and pepsin digested atelocollagen from fetal calf skin was acquired in lyophilized form from arGentis Collagen Labs (Memphis, USA). To demonstrate the purity of both extractions, an SDS-PAGE analysis was conducted with 4% stacker and 7.5% resolver, and stained with Coomassie Brilliant Blue (Fig. 1). All reagents used in this study were supplied from Sigma-Aldrich® (Poole, Dorset, UK) and all consumables were supplied from Fisher Scientific (Loughborough, Leicestershire, UK).

Type I collagen air-dried films were prepared from acid solubilized tropocollagen (T) and pepsin digested atelocollagen (A) in both afibrillar (af) and reconstituted fibrillar (rf) forms. The introduction of crosslinks using EDC/NHS into each type of sample resulted in eight different Type I collagen ultrastructures available for analysis. These ultrastructural combinations are summarized in Table 1.

To manufacture samples, collagen solutions were first prepared as described previously by Wahl [4]. Briefly, supplied lyophilized collagens were homogenized and completely dissolved in dilute ethanoic acid (pH 3.2), to make a 1% weight-to-volume solution. Air bubbles were then removed though centrifugation at 5,000 rpm (Thermo Electron Corporation IEC CL10) to create a monomeric solution. To produce afibrillar film samples, a thin layer of this monomeric collagen solution was spread onto the inner surface of a Petri dish and left to dry at room temperature.

Monomeric collagens in solution were also induced to polymerize through self-assembly and form fibrils in vitro. To create the conditions necessary for fibrillogenesis, monomers firstly needed to be moved to a neutral salt solution via dialysis. A 10 ml sample of 1 wt% monomeric collagen dissolved in dilute ethanoic acid was syringed into dialysis tubing (Spectra/Por 4 dialysis tubing, 12–14 K MWCO, 45 mm flat-width). This was dialysed against 1 l of *tris*-buffered saline (TBS) solution (50 mM *tris*-(hydroxymethyl)-aminomethane, 150 mM sodium chloride, pH 7.4) at 4°C for 12 h, three times. The monomeric collagen, now dissolved in TBS, was then removed from the dialysis tubing and syringed into a test tube. This was promptly placed into an incubator at 37°C for 4 h to allow the formation of a fibrillar gel pellet. The pellet was then removed and sliced with a scalpel into segments which were placed into a 1 l beaker of de-ionized water and left

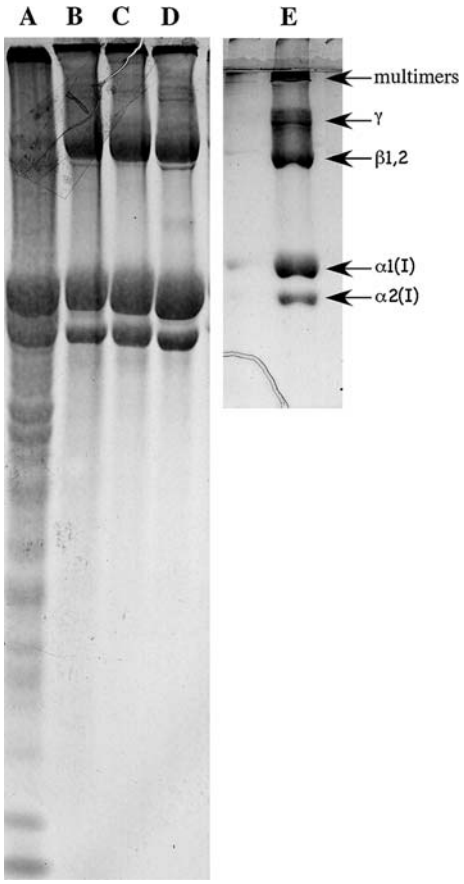

Fig. 1 SDS-PAGE of collagen extractions using 4% stacker, 7.5% resolver and stained with Coomassie Brilliant Blue, indicating the α1, α2(I), β1, 2, γ and multimer separations. Each band represents 60 μg of sample loaded onto the gel. A–D: pepsin digested atelocollagen, run on 23 cm slab gel. A = intermediate step in the purification process, B and D = final product supplied. C = reference atelocollagen from another purification. E: acid soluble tropocollagen supplied, run on 10 cm minigel

Table 1 Ultrastructural combinations of Type I bovine collagen samples

	Tropocollagen (T) Acid solubilized	Atelocollagen (A) Pepsin digested
Afibrillar (af)	afT	afA
	afTX	afAX
Reconstituted Fibrillar (rf)	rfT	rfA
	rfTX	rfAX

Acronyms used throughout the text. "X" denotes an EDC/NHS crosslinked sample

stirring overnight—this removed much of the salts from the pellets. To produce reconstituted fibrillar samples, pellets were homogenised into a slurry, centrifuged to remove air bubbles, and left to air dry in a Petri dish.

2.2 EDC/NHS crosslinking of collagen

Samples were crosslinked in 400 ml de-ionized water with a concentration of 60 mM 1-ethyl-3-(3-dimethylaminopropyl)-carbodiimide (EDC) and 30 mM *N*-hydroxysuccinimide (NHS). After crosslinking, with a reaction time of 3 h, the samples were washed twice in 400 ml 0.1 M Na_2PO_4 for 4 h and twice in 400 ml deionized water for 1 h. Samples were then left to air dry in a Petri dish.

2.3 Atomic force microscopy analysis

To obtain images from the AFM, 1 cm^2 was cut from the collagen films and mounted on a Park Instruments AutoProbe Atomic Force Microscope. Samples were scanned in Lateral Force Microscopy (LFM) mode with the force at 3 mN, with gain set to 0.3 and rate of 0.7 Hz

2.4 Fourier transform infra-red spectroscopy analysis

FTIR spectra were obtained from 1 cm diameter circular discs cut from collagen film samples. The discs were mounted in an FTIR sample holder between two translucent KBr discs. The sample was then scanned in a Perkin–Elmer Spectrum 2000 FT-IR Spectrometer from 4,000 to 400 cm^{-1} 150 times with the background scan subtracted.

2.5 Differential scanning calorimetry analysis

Denaturation temperatures of the samples were obtained using Mettler Toledo DSC821^e DSC and STAR^e software version 5.00. Using a mass balance, 6 mg of each collagen sample was weighed and hermetically sealed with 20 µl of deionized water in a standard Perkin–Elmer 40 µl aluminum test pan. A heating rate of 5°C/min was applied over the temperature range 20–90°C, with an empty aluminum pan as the reference probe. The endothermic transition was recorded graphically, from which peak denaturation temperature measurements were taken (T_d). Mean values of T_d for each sample were then calculated, where $n = 5$.

2.6 Enzymatic stability assay

The resistance of collagen samples to Type I bacterial collagenase from *Clostridium histolyticum* was determined experimentally. The protocol used was based on that of Wahl [4] and Angele [37]. Solutions of 0.1 M Tris-HCL, 0.05 M $CaCl_2$ at pH 7.4 (solution A), 0.1 M Tris-HCL and 100 units/ml of collagenase (solution B) and 0.25 M EDTA in dilute NaOH at pH 9.0 (solution C) were prepared. Each collagen sample was fashioned into a 5 mg pellet and placed in a 2 ml centrifuge tube (Eppendorf). To each centrifuge tube, 1 ml of solution A was added and the tubes were put into a shaking bath at 1 Hz, 37°C for 30 min. Then 1 ml of solution B was added and the samples were returned to the shaking bath for a further 1 h. To stop the reaction, 0.2 ml of EDTA was then added to the samples in an ice bath. Samples were then centrifuged at 15,000 rpm for 10 min (MSE HAWK 15/05 Centrifuge) and the supernatant removed using a pipette. Afterwards, 2 ml of deionized water was pipetted into each tube; they were then vortexed (IKA® MS2 Minishaker) and centrifuged again for 10 min at 15,000 rpm. This washing procedure was repeated 3 times overall with water and a further 3 times with ethanol. Samples were then left to air dry in a laminar flow cabinet and their final weight was measured. This procedure allows the mean percentage mass of collagen lost from a sample over the period of 1 h to be calculated, where $n = 3$. A control experiment was also carried out with all solutions and quantities kept the same but with the omission of collagenase to solution B.

2.7 Statistical analysis

DSC and enzymatic stability results are presented as the mean ± SD. One factor analyses of variance (ANOVA) with Fisher's LSD post-hoc test was performed using Origin® 8.0 software for Windows. Significance was accepted at a level of $P < 0.05$ for the DSC and enzymatic stability results.

3 Results

3.1 Atomic force microscopy results

AFM and Lateral Force Microscopy (LFM) images were obtained of all samples in ambient conditions to give visual information regarding their ultrastructure. AFM contact and tapping mode images showed poor detail and fibrils were not clearly defined in the images. However, using LFM, images could be obtained that showed enough detail and definition to observe fibrils in reconstituted fibrillar samples. LFM images are presented in Fig. 2. Afibrillar collagens showed only the balling-up of the surface, typical of an air-dried, globular protein (Fig. 2a). Reconstituted fibrils exhibited a diameter of ~100 nm (Fig. 2b). Monitoring the length of collagen fibrils using AFM/LFM was deemed unfeasible due to the three-dimensional weaved-lattice arrangement of fibrils, hindering observation of the termini.

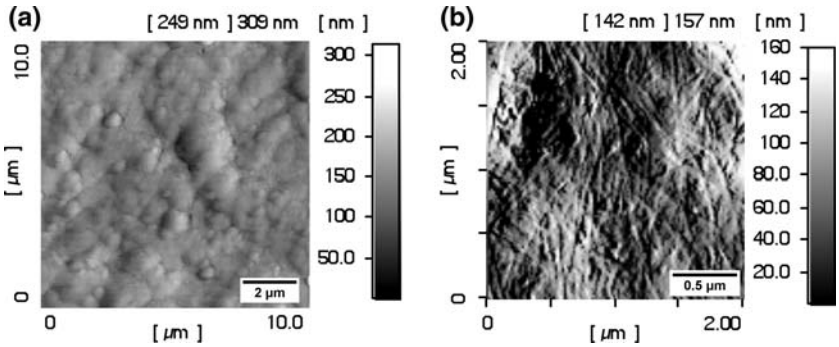

Fig. 2 LFM images of **a** uncrosslinked afibrillar atelocollagen (afA), which shows the balling-up of the surface and lack of fibrillar ultrastructure, and **b** crosslinked reconstituted fibrillar tropocollagen (rfTX), demonstrating the weaved-lattice arrangement of fibrils. All samples were scanned with 3mN force, 0.3 gain and 0.7 Hz rate

3.2 Fourier transform Infra-Red spectroscopy results

FTIR spectra of air-dried film samples all showed characteristic collagen Amide A, I, II and III peaks. Peak wavenumbers of these regions are given in Table 2. The spectra obtained from afibrillar and reconstituted fibrillar samples in uncrosslinked form (afT, afA, rfT, rfA) are all directly comparable in wavenumber, intensity and peak ratios. This suggests that FTIR is unable to distinguish between these ultrastructural differences when samples are in air-dried form. Afibrillar crosslinked samples (afTX, afAX), however, showed a decrease in intensity of the amide I and II region and a slight broadening of the amide I region relative to their uncrosslinked counterparts (Fig. 3). It should be noted though, that there was increased IR signal attenuation through these samples as the opacity of afibrillar crosslinked samples was the most pronounced.

Table 2 FTIR wavenumbers for Amide A, I, II, III characteristic peaks of all samples

	Peak wavenumber (cm^{-1})			
	Amide A	Amide I	Amide II	Amide III
Tropocollagen				
afT	3333.90	1652.31	1557.92	1240.04
afTX	3334.43	1652.31	1557.93	1240.50
rfT	3334.29	1652.33	1557.94	1239.59
rfTX	3322.62[a]	1652.32	1557.93	1239.69
Atelocollagen				
afA	3329.59	1652.29	1557.86	1240.05
afAX	3391.76[a]	1652.32	1557.93	1242.80[a]
rfA	3333.84	1652.28	1557.89	1239.94
rfAX	3334.07	1652.31	1557.91	1239.41

"X" denotes a crosslinked sample

af Afibrillar, *rf* Reconstituted fibrillar, *T* Tropocollagen, *A* Atelocollagen

[a] Denotes a shift in wavenumber. Significant shifts are observed exclusively in rfTX (Amide A) and afAX (Amide A, Amide III) samples

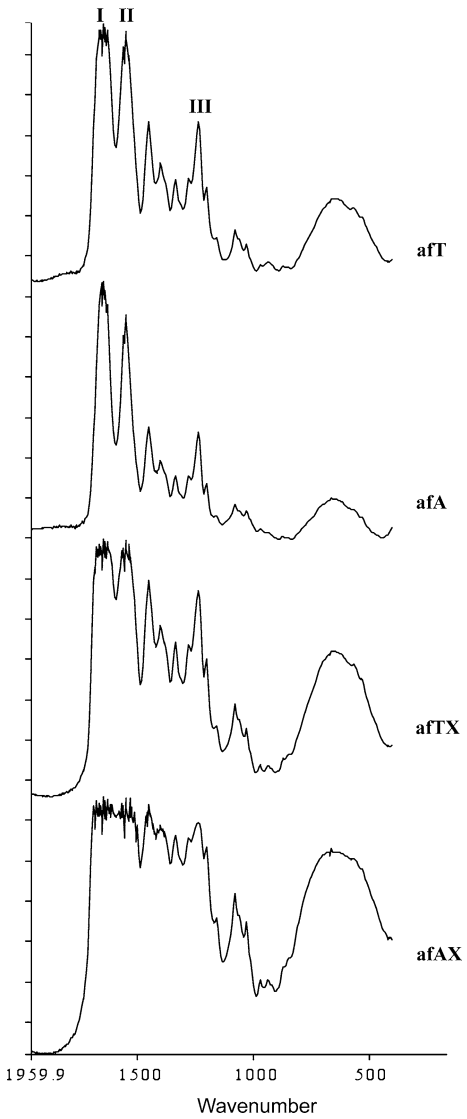

Fig. 3 FTIR Spectra, of afibrillar uncrosslinked/crosslinked samples with characteristic amide I, II and III peaks indicated (af = Afibrillar, T = Tropocollagen, A = Atelocollagen, "X" denotes a crosslinked sample). A decrease in intensity of the amide I and II regions and a slight broadening of the amide III region can be observed in crosslinked samples relative to uncrosslinked counterpart samples

3.3 Differential scanning calorimetry results

Using DSC, the hydrothermal stability of collagen samples was determined. Mean helix-to-coil transition temperatures (T_d) are presented ($n = 5$), with the standard deviation plotted as error bars (Fig. 4). Mean T_d (°C) recorded for uncrosslinked samples were: afT = 53.6, afA = 54.5, rfT = 56.2 and rfA = 55.2. Between uncrosslinked samples, the only statistically significant difference (mean difference of 2.6°C), is observed between afibrillar tropocollagen (afT) and reconstituted fibrillar tropocollagen (rfT). Mean T_d (°C) recorded for EDC/NHS crosslinked samples were: afTX = 80.7, afAX = 82.6, rfTX = 78.3 and rfAX = 78.8. These crosslinked samples showed a significant increase of ~27–28°C, in T_d for afibrillar samples (afTX, afAX) and ~22–24°C increase for reconstituted fibrillar samples (rfTX, rfAX). Overall, the behaviours of tropocollagen and atelocollagen samples are comparatively similar in these thermal stability analyses. However, it appears that the crosslinked, reconstituted fibrillar samples (rfTX, rfAX), were somewhat less able to reach the higher levels of thermal stability attained by the crosslinked, afibrillar samples (afTX, afAX).

3.4 Enzymatic stability assay results

The results of the enzymatic stability assays are presented in Fig. 5; significant differences between samples are as indicated above bars. The results of the control experiment showed no significant loss of material in solutions not containing collagenase. Consequently, all mean values of loss recorded were found to be significant compared with the control experiment ($P < 0.05$).

Dealing with the afibrillar samples first (afT, afA, afTX, afAX); crosslinked samples showed a significantly higher resistance to collagenase with only ~5–7% mean loss. Uncrosslinked afibrillar tropocollagen (afT) experienced a mean loss of 22.8%, and thus was >3.5 times more resistant to collagenase than counterpart atelocollagen samples (afA), which experienced a mean loss of 88.8% over the test period of 1 h.

Uncrosslinked, reconstituted fibrillar samples showed very low resistance to bacterial collagenase with an average loss of 86.1% for rfT and 98.4% for rfA. Again, when these samples were crosslinked, their resistance to degradation was significantly improved, albeit less so than for afibrillar samples.

The mean percentage loss differences between afibrillar and reconstituted fibrillar samples show that assembly into a fibrillar ultrastructure, for both tropocollagen and atelocollagen samples, reduces the resistance to collagenase; the most significant example being afT to rfT, where enzymatic stability is, on average, reduced by >3.5 times.

Overall, atelocollagen samples in all forms displayed less resistance, on average, to bacterial collagenase than counterpart tropocollagen samples.

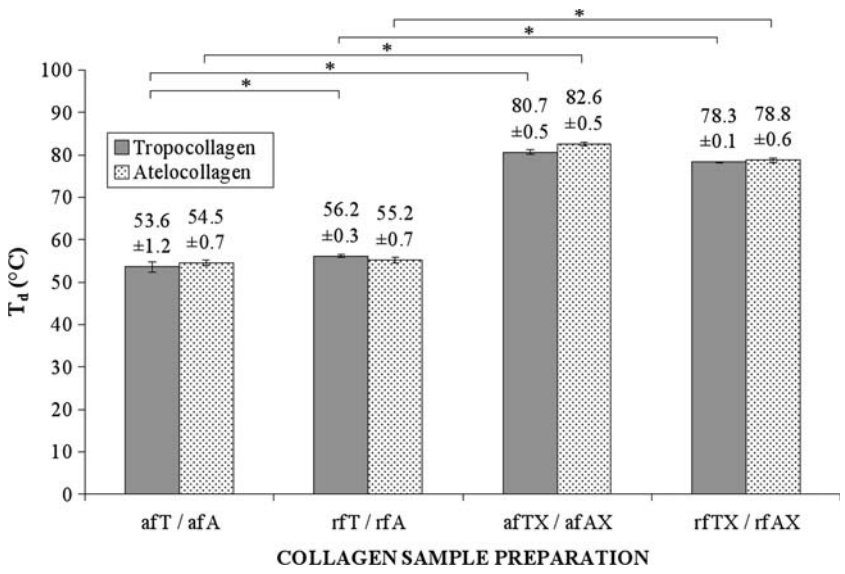

Fig. 4 Mean hydrothermal denaturation temperatures (T_d) of collagen samples, (af = Afibrillar, rf = Reconstituted Fibrillar, T = Tropocollagen, A = Atelocollagen, "X" denotes a crosslinked sample). * denotes a statistically significant difference between bars (Fisher's LSD post-hoc test, $P < 0.05$). A significant difference of 2.6°C is observed between afT and rfT, although, this was not found between counterpart afA and rfA samples. EDC/NHS crosslinked samples showed significantly higher denaturation temperatures compared to counterpart uncrosslinked samples. The values indicated represent mean ± SD, where $n = 5$

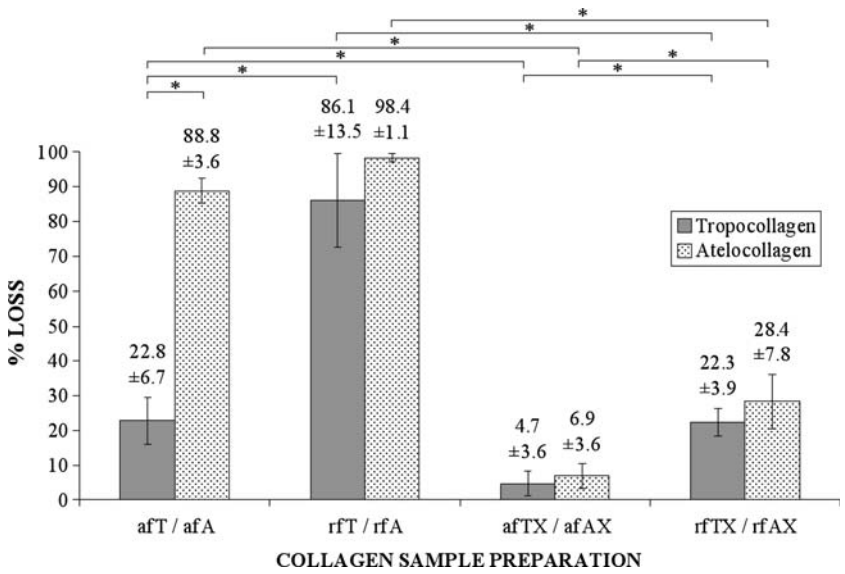

Fig. 5 Mean percentage loss of material from collagen samples during enzymatic stability assay (af = Afibrillar, rf = Reconstituted Fibrillar, T = Tropocollagen, A = Atelocollagen, "X" denotes a crosslinked sample). * denotes a statistically significant difference between bars (Fisher's LSD post-hoc test, $P < 0.05$). EDC/NHS crosslinking results in samples with improved resistance to enzymatic degradation. A significant difference in % loss is observed between afibrillar tropocollagen (afT) and afibrillar atelocollagen (afA) samples, as well as afT and rfT samples. The values indicated represent mean ± SD, where $n = 3$

4 Discussion

4.1 Lateral force microscopy

LFM images have provided evidence of a weaved-lattice network of fibrils with 100 nm diameters in reformed fibrillar samples that were formed from monomeric solutions and subjected to fibrillogenesis conditions (Fig. 2). These in vitro reconstituted fibrils have a notably thinner diameter to those found in vivo, which are of the order of 300–500 nm [55]. Afibrillar samples showed only an irregular balled up surface at the observed scale, however, other AFM studies have discovered a fine meshwork of monomers at higher magnification [56]. No significant differences could be observed between reconstituted fibrillar tropocollagen/reconstituted fibrillar atelocollagen samples using LFM. However, this is merely a limitation of observing matrices of air-dried, self-supported collagen fibrils in the AFM. Other electron microscope studies have elucidated the tactoidal, less-perfect packing order of atelocollagen fibrils [23–25]. From the LFM images of these samples, it is not possible to distinguish between tropo/atelo collagen samples and crosslinked/uncrosslinked samples. LFM, however, is a useful tool to quickly confirm an afibrillar/fibrillar ultrastructure and discern fibril diameters (if present) in air-dried collagen samples.

4.2 Fourier transform Infra-Red spectroscopy

The FTIR spectra has shown that the arrangement of collagen monomers from afibrillar into fibrillar ultrastructures has a negligible effect on the amide A, I, II and III peaks, when analysed as an air-dried film (Table 2). This result is incongruous with reported spectra that show distinct differences in these regions from samples analysed in solution [40–43]. The reason for this is likely to be as a direct result of the dehydration process, where the shrinkage of fibrils/triple helices and the extensive formation of intra and inter-molecular hydrogen bonds is attributed to the loss of water molecules. This shrinkage is expected to negate the ability of FTIR to detect differences in ultrastructure.

Crosslinked, afibrillar samples showed an increase in intensity of amide III and a broadening of amide I peaks compared to uncrosslinked counterparts. This signifies greater intermolecular interactions and increased hydrogen-bonding [57] (Fig. 3). These differences were not reflected in crosslinked fibrillar samples. It is most likely that the increased signal attenuation of afibrillar crosslinked samples is a factor for these substantial differences in spectra, especially considering the DSC results infer similar levels of crosslinking in fibrillar counterpart samples.

4.3 Differential scanning calorimetry

DSC results of the uncrosslinked samples showed comparatively small differences between mean T_d (Fig. 4). This demonstrates that the thermal behavior of afibrillar collagen samples at these high concentrations (300 g/l), where films are fully hydrated yet still intact, is more akin to fibrillar counterpart samples than monomeric collagens in true solution—where denaturation has been observed up to 20°C lower [58]. This behaviour may be explained by the polymer-in-a-box theory proposed by Miles et al., relating the spatial confinement of collagen molecules to the T_d [59]. Although originally proposed for fibrillar ultrastructures, hydrated afibrillar films with an irregular, layered ultrastructure are expected to provide a comparable amount of molecular spatial confinement to fibrillar counterpart samples—thus similar denaturation temperatures are observed. A statistically significant difference ($P < 0.05$), however, was found between afibrillar tropocollagen (afT) and reconstituted fibrillar tropocollagen (rfT) samples. Such differences were not observed between counterpart atelocollagen samples—thus fibrils formed in rfT samples are comparatively more hydrothermally stable. This behavior, again, can be attributed to higher molecular confinement in rfT fibrils compared to rfA fibrils, which have been reported to have a more perfect packing order [23–26]. In summary, the hydro-thermal behaviour of the uncrosslinked samples is ultimately related to the associated entropy of samples.

EDC/NHS crosslinking increased the hydrothermal stability of samples by a considerable amount. No significant differences were observed between the crosslinked tropo/atelo forms of each afibrillar/fibrillar sample. Afibrillar crosslinked samples (afTX/afAX), showed a slightly higher denaturation temperature compared to fibrillar samples, when crosslinked. Although deemed insignificant through the statistical analyses, this result is thought to be due to the crosslinking method used for afibrillar samples, in which crosslinking was carried out on air-dried films and not pellets—as described for reconstituted fibrillar samples. As a consequence, afibrillar samples inherently had a greater surface area exposed to crosslinking reagents thereby allowing greater access to crosslinking sites. Overall, the DSC results in this study demonstrate that the degree of molecular spatial confinement and the introduction of crosslinks has a direct influence on the denaturation temperature of hydrated collagen films. However, post-crosslinking, the technique has proved to be relatively insensitive to ultrastructural differences involving telopeptides and fibrils.

4.4 Enzymatic stability assay

Standard physicochemical analyses are only able to go so far in their effectiveness to distinguish between collagen ultrastructures. To fully consider the influence of telopeptides, fibrils and crosslinking, the biophysical implications of ultrastructure needed to be investigated. The enzymatic stability assay provided a simple in vitro laboratory test that has shown relevance to in vivo behaviors when characterizing collagen materials [54]. The results of this assay are discussed with respect to the physical properties found in this study.

From the enzymatic stability assay results (Fig. 5)—the observed difference between the mean percentage loss of afT and afA samples nicely demonstrates how the other physicochemical analyses used in this study were unable to distinguish between these two samples, yet a considerable difference is observed in their susceptibility to enzymatic attack. From this result, it appears that the presence of the telopeptide regions in the afT sample increases its resistance to collagenase by reducing the rate of enzymatic attack over the period of 1 h. It is widely believed that cleavage by collagenase depends largely on its ability to unwind the triple helix [50, 51]. A recent study by Perumal et al. [60], even postulates that removal of the C-terminal telopeptide is absolutely necessary as a first step, before collagenase can gain access to the cleavage site. As such, this result is most likely observed because the lack of telopeptide regions in the afA sample eliminates this first step in the degradation process. This enables the triple-helix to be unwound directly and then cleaved, resulting in a lowered activation energy and increased rate of reaction. Consequently, over the course of a 1 h reaction time, less intact material will remain from samples that lack a telopeptide region (afA).

The behaviours of the uncrosslinked collagen samples (afT, afA, rfT, rfA), when moving from an afibrillar to a fibrillar ultrastructure, was both interesting and unexpected. It appears that when the triple-helix collagen monomers are arranged into an ordered, fibrillar array with a $\sim$100 nm fibril diameter, the resistance to enzymatic attack is greatly decreased. This result, at first, appears to be in disagreement with other enzymatic degradation studies of monomeric/fibrillar collagens in true solution [61, 62]. However, this is the first study to directly compare hydrated, intact films of afibrillar/fibrillar collagens. In addition, the FTIR results in this study have also demonstrated that the differences between monomeric/fibrillar spectra described in true solution [40–43], were not observed in any collagen film samples. To help explain this phenomenon, it appears that the collagenase used in this assay is highly sensitive to the spatial arrangement of collagen monomers. As such, it is suggested that proximity between adjacent terminal ends in reconstituted fibrillar ultrastructures is key to the decrease in resistance, compared to afibrillar film samples. In one theory, hypothesised by Perumal et al. [60] on the action of collagenase, a lack

of crosslinkages at the terminus (as per uncrosslinked rf samples) may expose the α2 chain to cleavage, thereby allowing the remaining two chains greater movement. This could allow them to be twisted to face the catalytic domain and be proteolysed into αA (3/4 length) and αB (1/4 length) fragments. The subunits are then able to disassociate at physiological temperatures and are then susceptible to further degradation by collagenase [53]. Because of a lack of any significant crosslinking in the uncrosslinked fibrillar (rfT, rfA) samples in this study, it is suggested that local hydrogen-bond disturbances at the terminal ends of triple helices, induced by the presence and action of collagenase, affect adjacent terminal ends in fibrils in a mechanism similar to that hypothesised by Perumal et al., leading to additional cleavage. This proposed mechanism is presented diagrammatically in Fig. 6a. The overall effect of these proximity-induced-interactions leads to an increased rate of reaction and thus a higher amount of degradation is observed in fibrillar, uncrosslinked ultrastructures.

Uncrosslinked afibrillar samples have a globular macrostructure confirmed by LFM. At the molecular level, collagen molecules are randomly arranged and there is no specified alignment of side-groups or terminal ends. The whole structure is primarily held together by hydrogen-bonds formed during the dehydration process. Consequently, when treated with a solution of collagenase, and the telopeptide is cleaved (afT only), followed by the unzipping of the triple helix from the C-terminal end, there is much less likely to be a terminal end in close proximity that would be susceptible to hydrogen bond distortion (Fig. 6b). Thus, the increased degradation rate experienced by fibrillar ultrastructures via this proposed mechanism is not observed; in essence, the random-layered-lattice arrangement of monomers has a 'shielding' effect. Because of this, the percentage loss of material from afibrillar samples should be expected to be less than that of their reconstituted fibrillar counterparts.

4.5 Clinical implications

The results of this study indicate that differences in collagen ultrastructure, which may or may not be detectable by common materials characterization techniques, can have a profound effect on the enzymatic biodegradation properties of collagen. The two most important findings show that the presence of telopeptides can significantly hinder enzymatic degradation, and that uncrosslinked fibrillar ultrastructures are considerably more susceptible to enzymatic degradation than uncrosslinked afibrillar ultrastructures. Such phenomena may be utilized in the design process of tissue

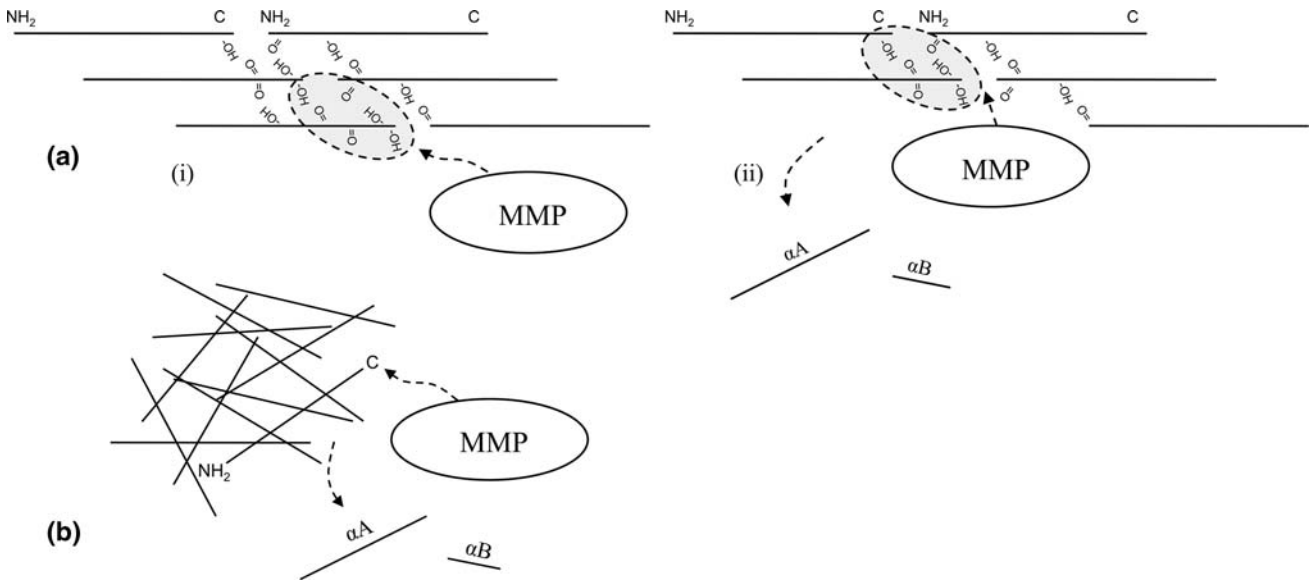

Fig. 6 **a** Proposed mechanism of collagenase action on uncrosslinked, reconstituted fibrillar ultrastructures; (i) Collagenase attacks the exterior of the fibril at the C-terminal of an individual collagen molecule. Local hydrogen bond disturbances are induced by the presence and action of collagenase in adjacent telopeptide regions (shown as grey shaded regions). (ii) The non-helical telopeptide region is removed (in tropocollagen only) and the enzyme is able to proceed to the helical cleavage site, leading to a triple α-chain scission (proteolysis fragments αA (3/4 length) and αB (1/4 length) are indicated). It is suggested that the close proximity of adjacent termini may induce additional cleavage during this process due to the lack of crosslinking and local hydrogen bond disturbances. **b** Proposed mechanism of collagenase action on uncrosslinked, afibrillar ultrastructures. The non-helical telopeptide region is removed (in tropocollagen only) and triple α-chain scission occurs (proteolysis fragments αA (3/4 length) and αB (1/4 length) are indicated). Due to the random-layered-lattice arrangement of monomers, however, proximity-induced hydrogen bond distortion at the termini of adjacent molecules is much less likely—thus additional cleavage via the mechanism proposed for reconstituted fibrillar ultrastructures (Fig. 6a), is not expected

engineering scaffolds. For example, hybrid afibrillar-fibrillar scaffolds may be fabricated to provide varying degrees of susceptibility to enzymatic attack in different scaffold regions. The use of these materials for such purposes would require further study on the influence of collagen ultrastructures on biological responses—specifically ligand-integrin cell attachment and the effects on cell phenotype. Additionally, the results of this study indicate that clinical biological data obtained using Type I collagen scaffolds of a defined ultrastructure may not be transferable to scaffolds fabricated from Type I collagen of differing ultrastructures, due to different physicochemical properties.

5 Conclusions

Collagen Type I has been prepared into eight distinct ultrastructures and subsequently analysed to demonstrate the influence of telopeptides, fibrils and crosslinking. LFM has proved to be a useful technique to confirm an afibrillar/fibrillar ultrastructure and to elucidate fibril diameters. The FTIR results have highlighted the inability of this method to distinguish between different ultrastructures in air-dried film form. However, intense crosslinking in afibrillar samples has provided some evidence of increased intermolecular interaction and hydrogen-bonding. DSC has demonstrated that the hydrothermal behaviour of hydrated afibrillar films is more akin to reconstituted fibrillar films than monomeric solutions. Crosslinking with EDC/NHS significantly increases the denaturation temperature of all samples. The limitation of DSC, however, is in distinguishing between different ultrastructures after crosslinking. The enzymatic stability assay indicated that tropocollagen samples were more resistant to collagenase than atelocollagen counterparts for the likely reason that telopeptide removal is necessary as a first step. Additionally, afibrillar films were found to be up to 3.5 times more resistant to bacterial collagenase than reconstituted fibrillar films, as a direct result of the different spatial arrangement of collagen molecules. This study has demonstrated the differences between these different Type I collagen preparations, highlighting the need for full disclosure of the source, extraction method, crosslinking and resultant ultrastructure when using these materials.

References

1. Lee CH, Singla A, Lee Y. Biomedical applications of collagen. Int J Pharm. 2001;221:1–22.
2. Sachlos E, Gotora D, Czernuszka JT. Collagen scaffolds reinforced with biomimetic composite nano-sized carbonate-substituted hydroxyapatite crystals and shaped by rapid prototyping to contain internal microchannels. Tissue Eng. 2006;12:2479–87.
3. Sachlos E, Reis N, Ainsley C, Derby B, Czernuszka JT. Novel collagen scaffolds with predefined internal morphology made by solid freeform fabrication. Biomaterials. 2003;24:1487–97.
4. Wahl D, Sachlos E, Liu C, Czernuszka J. Controlling the processing of collagen-hydroxyapatite scaffolds for bone tissue engineering. J Mater Sci Mater Med. 2007;18:201–9.
5. Sachlos E, Czernuszka JT. Making tissue engineering scaffolds work. Review: the application of solid freeform fabrication technology to the production of tissue engineering scaffolds. Eur Cells Mater. 2003;5:29–40.
6. Carmichael DJ, Lawrie RA. Bovine collagen I changes in collagen solubility with animal age. Int J Food Sci Technol. 1967;2:299–311.
7. Chang MC, Ikoma T, Kikuchi M, Tanaka J. Preparation of a porous hydroxyapatite/collagen nanocomposite using glutaraldehyde as a crosslinkage agent. J Mater Sci Lett. 2001;20:1199–201.
8. Cappabianca P, Esposito F, Cavallo LM, et al. Use of equine collagen foil as dura mater substitute in endoscopic endonasal transsphenoidal surgery. Surg Neurol. 2006;65:144–8.
9. Spira M, Liu B, Xu Z, Harrell R, Chahadeh H. Human amnion collagen for soft tissue augmentation—biochemical characterizations and animal observations. J Biomed Mater Res. 1994;28:91–6.
10. Olsen D, Yang C, Bodo M, et al. Recombinant collagen and gelatin for drug delivery. Adv Drug Deliv Rev. 2003;55:1547–67.
11. George J, Onodera J, Miyata T. Biodegradable honeycomb collagen scaffold for dermal tissue engineering. J Biomed Mater Res A. 2008;87A:1103–11.
12. Riemschneider R, Abedin MZ. Pepsin-solubilized collagen from cow placenta. Angew Makromol Chem. 1979;82:171–86.
13. Gross J, Kirk D. The heat precipitation of collagen from neutral salt solutions: some rate-regulating factors. J Biol Chem. 1958;233:355–60.
14. Steven FS. The presence of non-protein nitrogen in acetic acid-soluble calf-skin collagen. Biochem J. 1962;83:240.
15. Einbinder J, Schubert M. Binding of mucopolysaccharides and dyes by collagen. J Biol Chem. 1951;188:335–41.
16. Steven FS. Purification and amino acid composition of monomeric and polymeric collagens. Biochem J. 1967;104:534.
17. Grant ME. Carbohydrate content of bovine collagen preparations. Biochem J. 1968;108:587.
18. Eyre DR, Paz MA, Gallop PM. Cross-linking in collagen and elastin. Annu Rev Biochem. 1984;53:717–48.
19. Woodley DT, Yamauchi M, Wynn KC, Mechanic G, Briggaman RA. Collagen telopeptides (cross-linking sites) play a role in collagen gel lattice contraction. J Invest Dermatol. 1991;97:580–5.
20. Kadler KE, Hojima Y, Prockop DJ. Assembly of collagen fibrils de novo by cleavage of the Type I pC-collagen with procollagen C-proteinase. Assay of critical concentration demonstrates that collagen self-assembly is a classical example of an entropy-driven process. J Biol Chem. 1987;262:15696–701.
21. Gale M, Pollanen MS, Markiewicz P, Goh MC. Sequential assembly of collagen revealed by atomic force microscopy. Biophys J. 1995;68:2124–8.
22. Helseth DL Jr, Veis A. Collagen self-assembly in vitro. Differentiating specific telopeptide-dependent interactions using selective enzyme modification and the addition of free amino telopeptide. J Biol Chem. 1981;256:7118–28.
23. Brennan M, Davison PF. Influence of the telopeptides on Type I collagen fibrillogenesis. Biopolymers. 1981;20:2195–202.

24. Comper WD, Veis A. The mechanism of nucleation for in vitro collagen fibril formation. Biopolymers. 1977;16:2113–31.
25. Leibovic SJ. Electron microscope studies of effects of endopeptidase and exopeptidase digestion on tropocollagen. Biochim Biophys Acta. 1970;214:445.
26. Zeugolis DI, Paul RG, Attenburrow G. Factors influencing the properties of reconstituted collagen fibers prior to self-assembly: animal species and collagen extraction method. J Biomed Mater Res A. 2008;86A:892–904.
27. Lynn AK, Yannas IV, Bonfield W. Antigenicity and immunogenicity of collagen. J Biomed Mater Res B Appl Biomater. 2004;71B:343–54.
28. Klein AW. Tissue augmentation in clinical practice. 1st ed. New York: Marcel Dekker; 1998.
29. Cao H, Xu S-Y. EDC/NHS-crosslinked Type II collagen-chondroitin sulfate scaffold: characterization and in vitro evaluation. J Mater Sci Mater Med. 2008;19:567–75.
30. McPherson JM, Sawamura S, Armstrong R. An examination of the biologic response to injectable, glutaraldehyde cross-linked collagen implants. J Biomed Mater Res. 1986;20:93–107.
31. Sionkowska A, Kaminska A. Thermal helix-coil transition in UV irradiated collagen from rat tail tendon. Int J Biol Macromol. 1999;24:337–40.
32. Rabotyagova OS, Cebe P, Kaplan DL. Collagen structural hierarchy and susceptibility to degradation by ultraviolet radiation. Mater Sci Eng C. 2008;28:1420–9.
33. Speer DDP, Chvapil MM, Eskelson CCD, Ulreich JJ. Biological effects of residual glutaraldehyde in glutaraldehyde-tanned collagen biomaterials. J Biomed Mater Res. 1980;14:753–64.
34. Weadock KS, Miller EJ, Keuffel EL, Dunn MG. Effect of physical crosslinking methods on collagen-fiber durability in proteolytic solutions. J Biomed Mater Res. 1996;32:221–6.
35. Weadock KS, Miller EJ, Bellincampi LD, Zawadsky JP, Dunn MG. Physical crosslinking of collagen fibers: Comparison of ultraviolet irradiation and dehydrothermal treatment. J Biomed Mater Res. 1995;29:1373–9.
36. Thompson JI, Czernuszka JT. The effect of two types of crosslinking on some mechanical properties of collagen. Bio-Med Mater Eng. 1995;5:37–48.
37. Angele P, Abke J, Kujat R, et al. Influence of different collagen species on physico-chemical properties of crosslinked collagen matrices. Biomaterials. 2004;25:2831–41.
38. Lee JM, Edwards HHL, Pereira CA, Samii SI. Crosslinking of tissue-derived biomaterials in 1-ethyl-3-(3-dimethylaminopropyl)-carbodiimide (EDC). J Mater Sci Mater Med. 1996;7:531–41.
39. Christiansen DL, Huang EK, Silver FH. Assembly of Type I collagen: fusion of fibril subunits and the influence of fibril diameter on mechanical properties. Matrix Biol. 2000;19:409–20.
40. Milch RA. Aqueous solution infrared spectra of collagen-reactive aldehydes. Biochim Biophys Acta. 1964;93:45–53.
41. Jakobsen RJ, Brown LL, Hutson TB, Fink DJ, Veis A. Intermolecular interactions in collagen self-assembly as revealed by Fourier transform infrared spectroscopy. Science. 1983;220:1288–90.
42. George A, Veis A. FTIRS in water demonstrates that collagen monomers undergo a conformational transition prior to thermal self-assembly in vitro. Biochemistry. 1991;30:2372–7.
43. Prystupa DA, Donald AM. Infrared study of gelatin conformations in the gel and sol states. Polym Gels Networks. 1996;4:87–110.
44. Paschalis EP, Verdelis K, Doty SB, Boskey AL, Mendelsohn R, Yamauchi M. Spectroscopic characterization of collagen crosslinks in bone. J Bone Miner Res. 2001;16:1821–8.
45. Foltran I, Roveri EFBPPSN. Novel biologically inspired collagen nanofibers reconstituted by electrospinning method. Macromol Symp. 2008;269:111–8.
46. Friess W, Lee G. Basic thermoanalytical studies of insoluble collagen matrices. Biomaterials. 1996;17:2289–94.
47. Kopp JJ, Bonnet MM, Renou JJP. Effect of collagen crosslinking on collagen-water interactions (a DSC investigation). Matrix. 1989;9:443–50.
48. Flandin F, Buffevant C, Herbage D. A differential scanning calorimetry analysis of the age-related changes in the thermal stability of rat skin collagen. Biochim Biophys Acta. 1984; 791:205–11.
49. Ala-aho R, Kähäri V-M. Collagenases in cancer. Biochimie. 2005;87:273–86.
50. Chung L, Dinakarpandian D, Yoshida N, et al. Collagenase unwinds triple-helical collagen prior to peptide bond hydrolysis. EMBO J. 2004;23:3020–30.
51. Tam EM, Moore TR, Butler GS, Overall CM. Characterization of the distinct collagen binding, helicase and cleavage mechanisms of matrix metalloproteinase 2 and 14 (gelatinase A and MT1-MMP): the differential roles of the MMP hemopexin C domains and the MMP-2 fibronectin Type II modules in collagen triple helicase activities. J Biol Chem. 2004;279:43336–44.
52. von Heimburg D, Zachariah S, Kühling H, et al. Human preadipocytes seeded on freeze-dried collagen scaffolds investigated in vitro and in vivo. Biomaterials. 2001;22:429–38.
53. Sakai T, Gross J. Some properties of the products of reaction of tadpole collagenase with collagen. Biochemistry. 1967;6:518–28.
54. Yannas IV, Burke JF, Huang C, Gordon PL. Correlation of in vivo collagen degradation rate with in vitro measurements. J Biomed Mater Res. 1975;9:623–8.
55. Hong S, Hong S, Wallace J, Kohn D. Ultrastructural observation of electron irradiation damage of lamellar bone. J Mater Sci Mater Med. 2009;20:959–65.
56. Chernoff EAG, Chernoff DA. Atomic force microscope images of collagen fibers. J Vac Sci Technol A. 1992;10:596–9.
57. Muyonga JH, Cole CGB, Duodu KG. Fourier transform infrared (FTIR) spectroscopic study of acid soluble collagen and gelatin from skins and bones of young and adult Nile perch (Lates niloticus). Food Chem. 2004;86:325–32.
58. Leikina E, Mertts MV, Kuznetsova N, Leikin S. Type I collagen is thermally unstable at body temperature. Proc Natl Acad Sci USA. 2002;99:1314–8.
59. Miles CA, Ghelashvili M. Polymer-in-a-box mechanism for the thermal stabilization of collagen molecules in fibers. Biophys J. 1999;76:3243–52.
60. Perumal S. Collagen fibril architecture, domain organization, and triple-helical conformation govern its proteolysis. Proc Nat Acad Sci USA. 2008;105:2824.
61. Netzel-Arnett S, Fields GB, Birkedal-Hansen H, Van Wart HE, Fields G. Sequence specificities of human fibroblast and neutrophil collagenases. J Biol Chem. 1991;266:6747–55.
62. Leibovich SJ, Weiss JB. Failure of human rheumatoid synovial collagenase to degrade either normal or rheumatoid arthritic polymeric collagen. Biochim Biophys Acta. 1971;251:109–18.